FATIGUE AND CREEP PROPERTIES IN RELATION

WITH ALLOY 718 MICROSTRUCTURE

B. Pieraggi and J.F. Uginet*

Laboratoire des Matériaux-URA 445 CNRS
ENSCT-INPT
31077 Toulouse Cedex, France
* FORTECH-Division AirForge
BP
Pamiers Cedex, France

Abstract

The effect of microstructural parameters such as grain size, size and distribution of carbide or nitride inclusions, shape and distribution of δ-precipitates, on the fatigue and creep properties of Alloy 718 was investigated. The investigations and analysis was performed on a large number of test pieces coming from required control or qualification tests of forged gas turbine discs. Grain size and shape and distribution of δ-precipitates are the most important parameters to control fatigue and creep behavior respectively.

Superalloys 718, 625, 706 and Various Derivatives
Edited by E.A. Loria
The Minerals, Metals & Materials Society, 1994

Introduction

Creep and fatigue behavior of 718 Alloy depends strongly on its microstrucuture. The effect of grain size is well recognized but this effect differs for creep and fatigue : grain sizes of 4 to 6 ASTM index favor creep resistance while smaller grain sizes (ASTM index between 9 to 12) improve fatigue life. However, several additional factors linked to microstructural features also affect the mechanical properties of 718 Alloy forging parts.

Therefore, the goal of the present work was to analyze the effect of :

- grain size
- morphology and density of δ-$NiNb_3$ precipitates
- carbide or nitride distribution
- dislocation density
- density of hardening precipitates

on the creep and fatigue properties of forging parts, usually gas turbine discs, looking for the best compromise between creep and fatigue, although fatigue behaviour is usually predominant in gas turbine applications.

Most of the examined test pieces come from required control tests of manufactured forged parts. However, some additional creep and fatigue tests were performed on small forged bars with specific microstructure. The knowledge of flow stress as a function of strain, strain rate and temperature, and of recrystallization kinetics (1), permits to obtain materials with the desired microstructure from fine-grained to coarse-grained or duplex microstructures.

All the investigations were performed on test pieces submitted to practical and usual fatigue and creep control tests required in usual control procedures of gas turbine discs. Data from more than one hundred fatigue tests and an identical number of creep or stress rupture tests were collected and analyzed, and correlated to the previously mentionned microstructural factors.

Materials and experimental methods

Most of the examination were performed on test pieces machined from cut ups and test ring of forged discs. VIM/VAR billets 150 to 300 mm in diameter were the usual starting materials. The composition of these billets was always in the following limits for the major addition elements : $5.2<Nb+Ta<5.4$, $17.5<Fe<18.5$, $2.9<Mo<3.0$, $0.90<Ti<1.05$ and $0.40<Al<0.60$. Specific tests were performed from cylindrical bars deformed parallel to their longitudinal axis which leads to a relatively large zone of homogeneous microstructure. After forging, all parts are heat-treated at 970 °C before the usual double aging at 720 and 620 °C.

Analyzed fatigue data cover a large fatigue life range . The test conditions were kept constant :

- frequency range between 0.1 and 0.5 Hz,
- stress ration R=0.05
- sinusoidal waveform (without holding time)
- constant total strain amplitude between 0.8 10^{-3} and 0.5 10^{-3}
- test temperatures between 350 and 550 °C.

Stress rupture and creep tests were performed between 650 and 700 °C under stresses from 400 to 730 MPa for stress rupture tests and 250 to 550 MPa for creep tests. Test durations were between 20 to 300 hours, all tests were stopped after 300 hrs. The tests were characterized by the rupture time or the test duration at a given elongation (usually between 0.1 and 0.2 %).

Metallographic examinations were always made on the undeformed head of fatigue and creep test pieces. They were performed on sections normal to the test piece axis. However, for some fatigue test pieces, metallographic examinations were carried out in a plane parallel to the test piece axis. These examinations permitted to relate more closely the crack propagation path to the specimen microstructure. TEM examinations of thin foils normal to the specimen axis and cut from the undeformed test pieces heads were also performed when required.

Fracture surface of fatigue and creep test pieces were systematically examined macroscopically or by SEM to determine the fracture mode, the specific characteristics of the fracture. For fatigue test pieces, the initiation site and mode of initiation was more specifically analyzed.

The micrographs of figure 1 are characteristic of fine-grained microstructures (figure 1a) and homogeneously dispersed globular δ precipitates (figure 1b) and of coarse-grained microstructures with acicular δ precipitates (figure 1c).

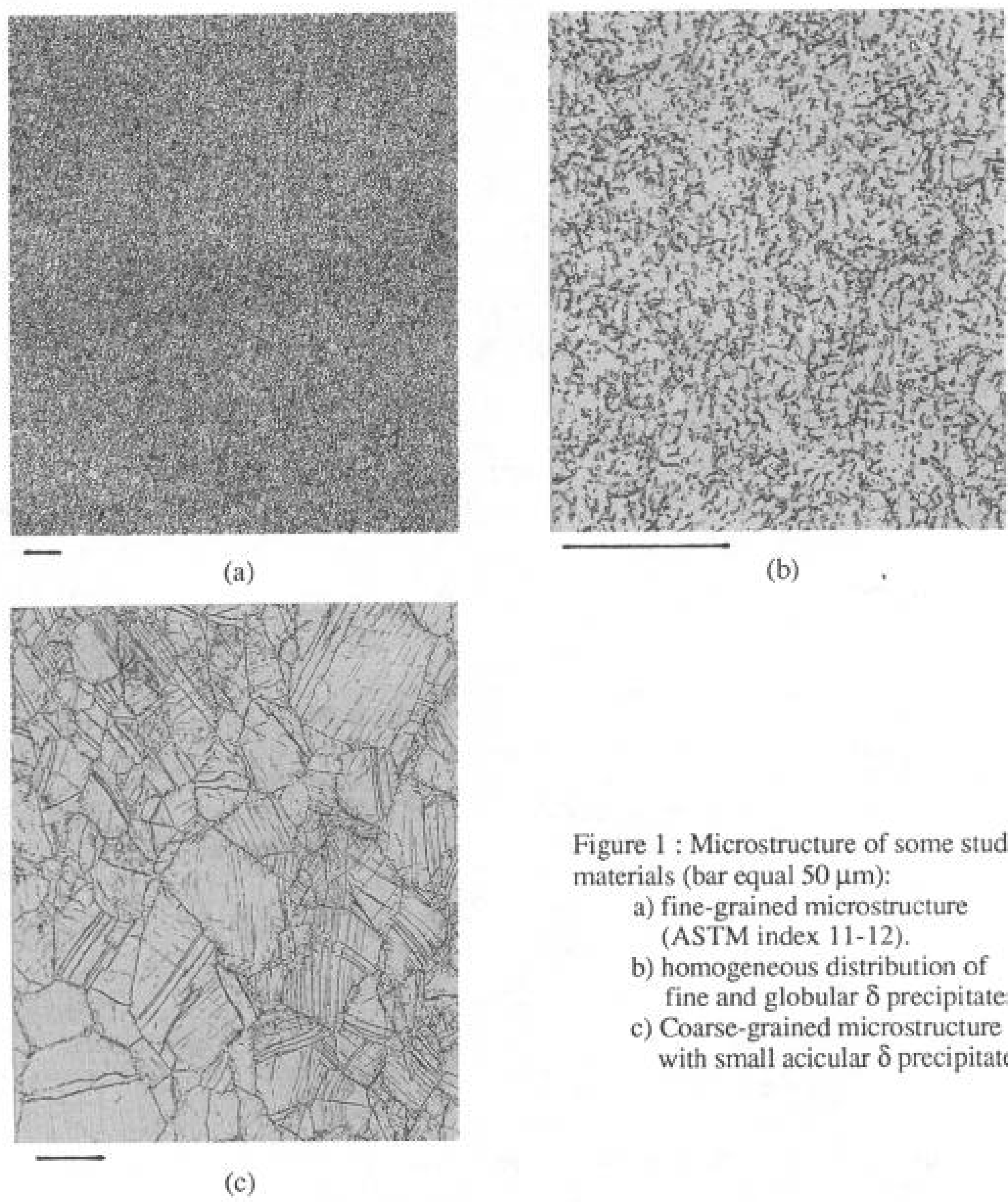

Figure 1 : Microstructure of some studied materials (bar equal 50 μm):
a) fine-grained microstructure (ASTM index 11-12).
b) homogeneous distribution of fine and globular δ precipitates.
c) Coarse-grained microstructure with small acicular δ precipitates

Fatigue tests

Fatigue properties are of particular importance for gas turbine discs. Among the performed investigations and analysis, grain size appears to be more important then the others invest igated parameters. No significant effect of shape and distribution of δ precipitates was observed

Effect of Grain Size

The effect of grain on fatigue properties is well illustrated by Figure 2 which shows the average variation of Nf, number of fatigue cycles to failure, or fatigue life, as a function of the maximun stress. This figure clearly indicates that, at 350 and 550 °C, a smaller grain size induces an improvement of fatigue life. These curves also show the usual effect of temperature on the fatigue life of 718 Alloy : for fatigue lifes higher than about 10^4 cycles, fatigue lifes at 550 °C are longer than at 350 °C as already observed by Sanders et al. (2).

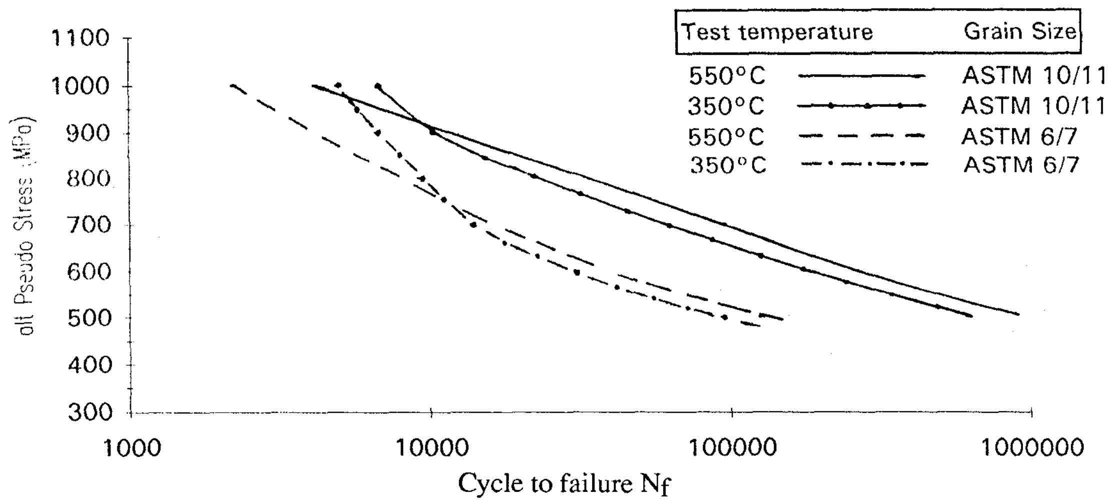

Figure 2 : Average fatigue curves for fine-grained specimens (ASTM index between 10 and 12) and coarse-grained specimen (ASTM index 6/7)

The microstructure of analysed test pieces can be classified into five classes :

- Microstructure 1 : homogeneous ASTM 6 + some 7/8
- Microstructure 2 : homogeneous ASTM 7/8 + some 8/10
- Microstructure3 : homogeneous ASTM 9 or 10 with less than 10% of 6/8 grains
- Microstructure 4 : homogeneous ASTM 10 to 12 with les than 10 % of 7/9 grains
- Microstructure 5 : duplex ASTM 9 or 10 with more than 20 % of 6/7 grains

For tests performed under constant strain conditions, the data can be fitted to the Basquin's law :

$$\frac{\Delta\sigma}{2} = \sigma'_f \cdot (2N_f)^b \qquad (1)$$

This law can be applied to microstructure 1 to 3. The value of σ'_f coefficients and b exponents are reported in Table 1.

Data reported in Table I show that the coefficient σ'_f does not vary significantly with microstructure and test temperature, but the absolute value of b exponent is higher at 350 °C than 550 °C and decrease with the grain size, so that for homogeneous fine-grained microstructures of ASTM 9/10, there is no difference in the coefficients of Basquin's law at 350 and 550 °C.

For specimens with a very fine-grained microstructure (microstructure 4) or duplex microstructure (microstructure 5), data could not be fitted to the Basquin's law, and appeared to be more dispersed and less reproducible than for specimens of classes 1 to 3. Moreover, the fatigue behavior of specimens with a duplex microstructure is similar to that of coarse-grained specimens as soon as the percentage of large grains exceeds 15 %

Table I : Coefficient of Basquin's law at 350 and 550 °C.

Temperature	Microstructure class	σ'_f	b
350 °C	1	$10^{3.30}$	- 0.11
	2	$10^{3.15}$	- 0.10
	3	$10^{3.00}$	- 0.05
550 °C	1	$10^{3.05}$	- 0.070
	2	$10^{3.10}$	- 0.075
	3	$10^{3.00}$	- 0.05

Crack Initiation

The fracture surface of numerous test pieces of the previously defined microstructure classes were systematically observed to determine crack initiation sites. Specimens of homogeneous microstructure of ASTM 6 or 7 (microstructure 1 or 2) are always characterized by a unique initiation site, corresponding to well defined crystallographic facets, as illustrated by Figure 3. The decrease in fatigue life of specimens with duplex microstructures comes from crack initiation at large grains. For specimens with homogeneous fine-grained microstructure (microstructure 5), several crack initiations are commonly observed, which explains that Basquin's law cannot apply. These multiple initiations are sometimes localized on carbide inclusions or under the specimen surface (Figure 4). Morever, tests performed on specimens from an VIM/ESR/VAR billet with likely a lower inclusion level did not show significant change in fatigue lifes and initiation sites.

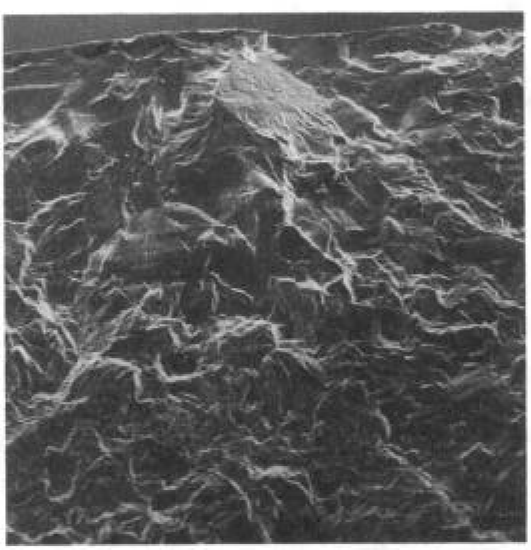

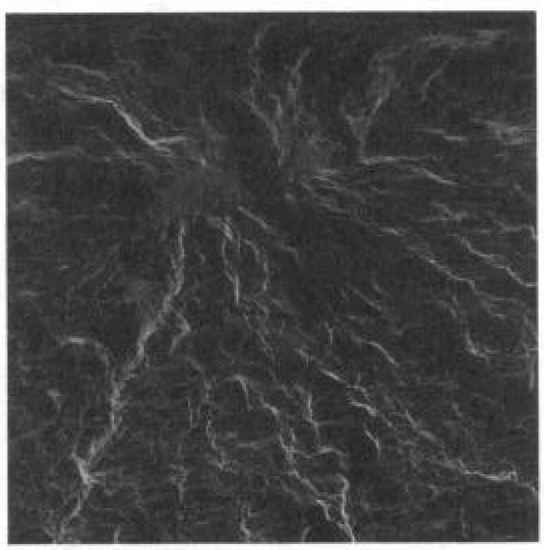

(bar equal 10 μm)

Figure 3 : Crystallographic initiation (microstructure 1, T=550 °C)

Figure 4 : Crack initiation under the specimen surface (microstructure 3, T=350 °C)

Crack Propagation

Metallographic examinations along a plane normal to the crack propagation, showed that the crack path, for specimens of microstrucutre 1 or 2, has a mixed intergranular and transgranular character with only few secondary cracks, as illustrated by Figure 5. The δ precipitates often interfere with the crack path depending on their shape and orientation.

Large Ti and Nb carbides or nitrides (up to 20 μm) were sometimes found on the rupture surface of all specimen classes. No apparent increase of striation spacing, i.e. of crack propagation rate, can be associated with these carbides. Specific morphology of the surface rupture, consisting in steps formed from sharp slip bands intersecting the carbide/alloy interface, are often observed (Figures 6 and 7). These observations show that these carbides, even of large size, have no real deleterious effect on crack initiation and propagation.

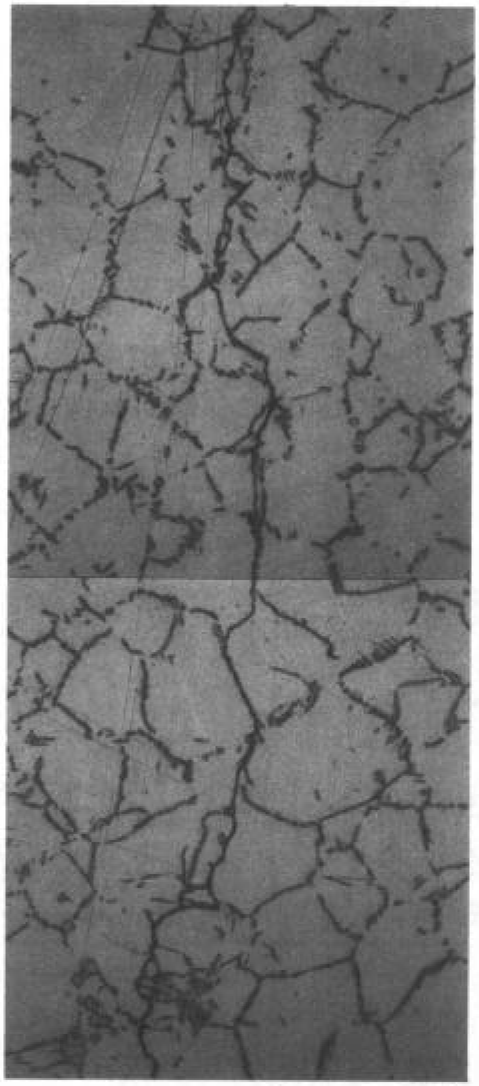

Figure 5 : Metallographic examinations showing intergranular and transgranular propagation.(Microstructure 1, T=550 °C, bar equal 50μm)

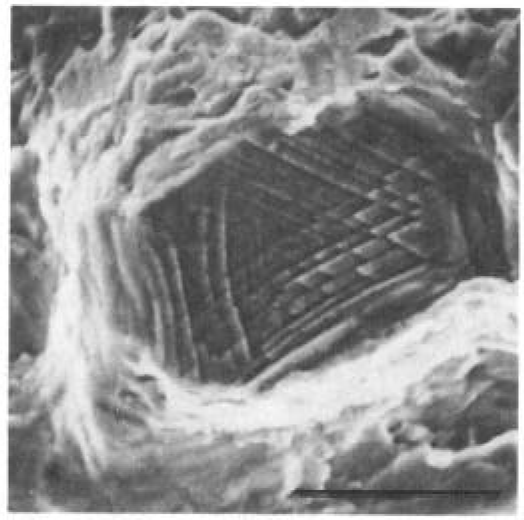

Figure 6 : Interfacial steps resulting from the intersection of sharp slip bands and large carbide (bar equal 10 μm).

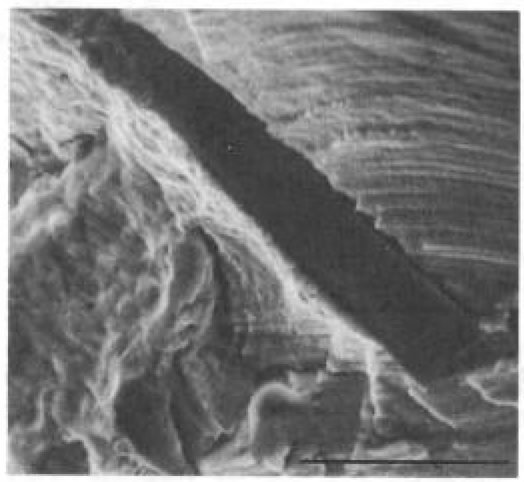

Figure 7 : Interfacials steps formed at the alloy/Ti-rich precipitates interface (bar equal 10 μm)

Creep tests

Stress Rupture Tests

Figure 8 summarizes the observed behavior by roughly correlating the time to rupture at 650 °C and 730 MPa to the average grain size of a homogeneous microstructure, the time to rupture decrease as the grain size decreases in agreement with the observation of crack growth rate inversely proportional to the grain size, as reported by Liu et al. (4). For a duplex microstructure, Figure 9 shows that the time to rupture increases with the amount of large grains.

At constant grain size, the size and morphology of δ precipitates are the most significant parameters. Globular δ precipitates leads to larger time to rupture, while acicular precipitates have a marked deleterious effect. For instance, with an homogeneous 9/10 grain size, the time to rupture at 650 °C and 690 MPa changes from 250 hours with globular δ precipitates to 70 hours with acicular δ precipitates.

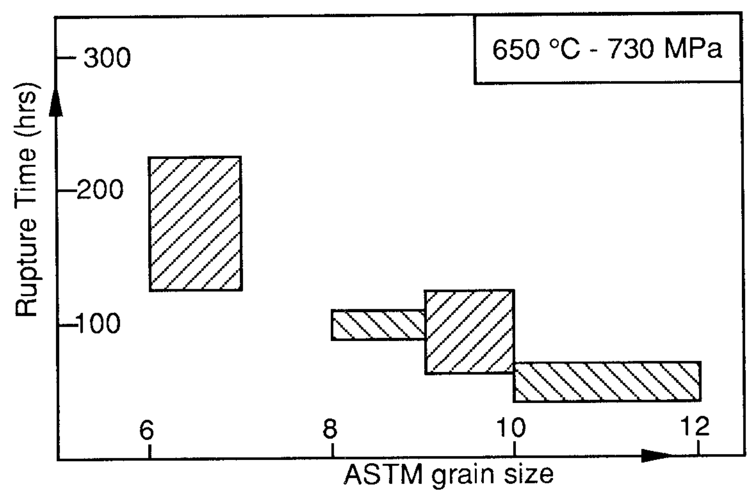

Figure 8 : Effect of grain size on the time to rupture (homogeneous microstructure).

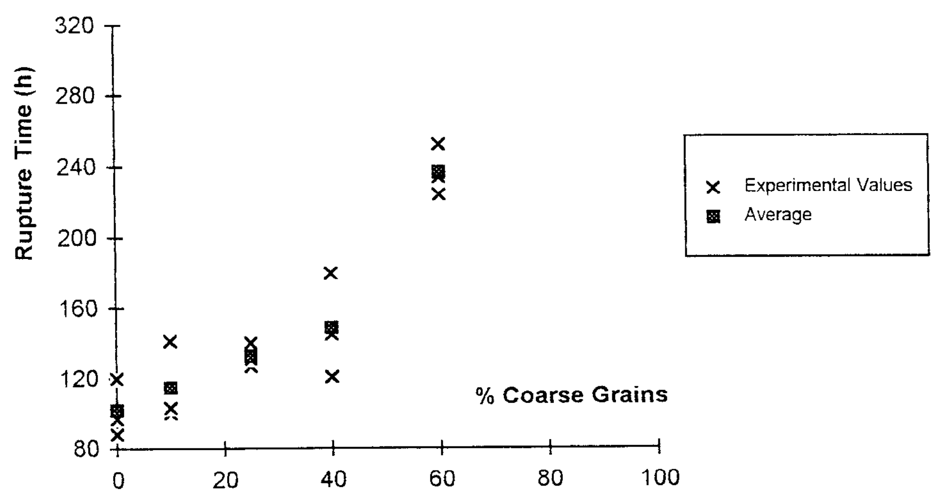

Figure 9 : Effect of the amount of large grains on the time to rupture (duplex microstructure).

The distribution of δ precipitates is also an important parameter. As already observed by Pedron and Pineau (5), intergranular δ precipitates drastically improve the behavior of notched test pieces. For instance, for the same test conditions the time to rupture of test pieces, corresponding to the microstructures illustrated by Figures 10 a-b, changes from less than 2 hours to 255 hours, although the grain size of the specimen with intergranular δ is smaller. The distribution, size and shape of carbides or nitrides was systematically examined, but no apparent or significant effect was detected.

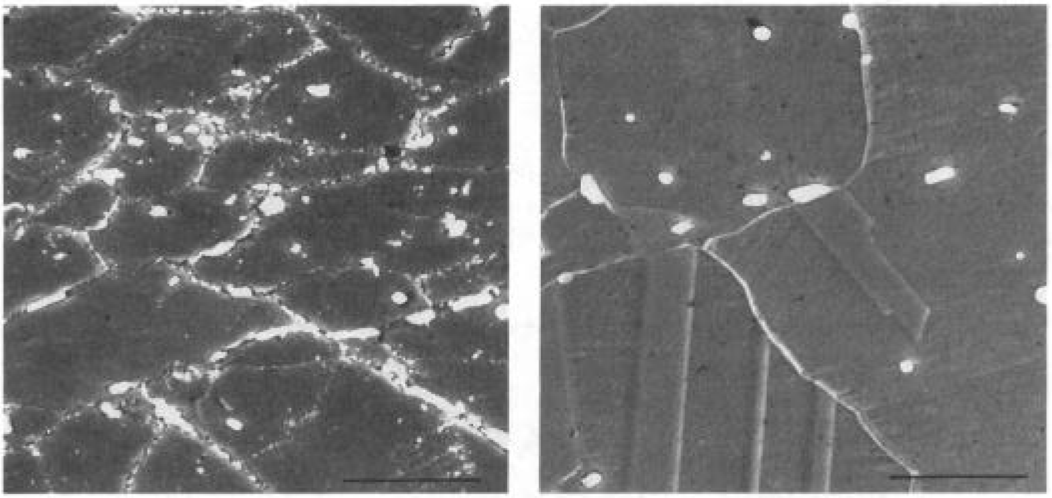

(a) (b)

Figure 10 : Microstructure of specimens withe globular d precipitates (bar equal 10 μm)
- a) intergranular distribution b) transgranular distribution

Creep Tests

Within the limits of the studied microstructures, no correlation was found between the grain size and the observed elongation for test duration between 15 to 300 hours. Similarly, no clear influence of shape, density and distribution of δ precipitates was observed.

For example, Table II summarizes the creep data obtained at 705 °C and 250 MPa on similar test pieces characterized by a fine and homogeneous 9/11 grain size with evenly distributed globular δ precipitates.

A and B specimens come from two different forged parts and thus from different heats. The chemical compositions of A and B specimen are similar, the main difference is the Fe content which changes from 18.5 to 17.5 for A and B respectively

Table II : Elongation and creep rate at 705 °C and 250 MPA

Specimen	% Elongation after 15 hours	% Elongation after 100 hours	Time to 0.2 % elongation	Average Creep Rate between 15 and 100 hrs.
A3	0.03	0.14	132	$1.3\ 10^{-3}$
A4	0.11	0.17	161	$0.7\ 10^{-3}$
B7	0.05	0.15	145	$1.1\ 10^{-3}$
B11	0.12	0.41	40	$3.4\ 10^{-3}$

TEM examinations (Figure 11) performed on the undeformed part of four test pieces (A3, A4, B7 and B11) permit the following observations :

- the specimen B11 is characterized by a large dislocation density
- the density of hardening precipitates is higher in A3 and A4 specimens (about 2000 preciptates/mm^2) than in B7 and B11 specimens (about 1200 precipitates/mm^2).

This difference in hardening precipitate density between A and B specimen cannot explain the variation in creep behavior shown by Table II.

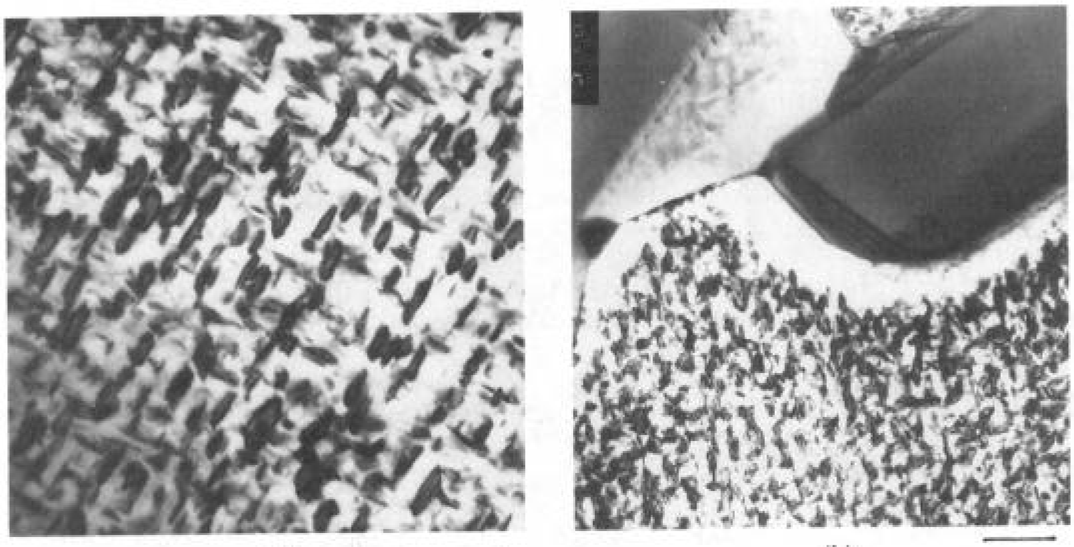

(a) (b)

Figure 11 : TEM examination of the microstructure of undeformed parts of creep specimens
a) density and distribution of hardening precipitates (bar equal 0.1 μm)
b) depletion in hardening precipitates along grain boundary with δ intergranular precipitates (bar equal 0.2 μm)

These TEM examinations showed that the intergranular precipitation of δ Ni_3Nb always induces the formation of a narrow zone depleted in hardening precipitates along the grain boundaries (Figure 11b). The formation of these depleted zones may explain the beneficial influence of intergranular δ precipitates on crack propagation.

Conclusions

The present work was focused on the microstructure usually required for engine disc applications and practical control tests (qualification parts and routine tests). Thus, the range of investigated microstrucutre was limited to the grain sizes between ASTM 6/7 to ASTM 10/12.

The reported data show that the grain size is effectively the most important parameter for both fatigue and creep behavior. Standard average curves showing the effect of grain size on fatigue life and stress rupture were determined from the analysis of a large number of test specimens.

Grain size appeared as the most important parameter to control the fatigue life from the materials microstructure. The shape, size or distribution of δ-precipitates have no apparent effect. Similarly, carbide or nitride inclusions do not appear to have a significant effect within the range of studied microstructure and test conditions.

Creep behavior is more difficult to describe. Indeed, both grain size and δ-precipitates can affect strongly the time to rupture or the creep rate. However, δ-precipitates seems to have a more pronounced effect than grain size, the presence of few acicular δ-precipitates can induce a drastic reduction in life if all the others parameters are kept constant. No apparent effect of carbide or nitride inclusions was observed.

References

1) G. Camus, B. Pieraggi, and F. Chevet, "Hot Deformation and Recrystallization of Inconel 718", Formability and Metallurgical Structure, ed. A.K. Sachdev and J.D. Embury (Warrendale, PA : The Metallurgical Society, 1987), 305-325

2) T.H. Sanders, Jr., R.E. Frishmuth, and G.T. Embley, "Temperature Dependent Deformartion Mechanisms of Alloy 718 in Low Cycle Fatigue", Metall. Trans., 12A (1981) 1003-1010

3) T. Denda, P.L. Bretz, and J.K. Tien, "Inclusion Size Effect on the Fatigue Crack Propagation Mechanism and Fracture Mechanics of a Superalloy", Metall. Trans., 23A (1992) 519-526

4) C.D. Liu, Y.F. Han, M.G. Yan, and M.C. Chaturvedi, "Creep Crack Growth Behaviour of Alloy 718", Superalloys 718-625, ed. by E.A. Loria, (Warrendale, PA : The Metallurgical Society, 1991), 537-547

5) J.P. Pedron and A. Pineau, "The effect of Microstructure and Environment on the Crack Growth Behaviour of Inconel 718 Alloy at 650 °C under Fatigue, Creep and Combined Loading", Materials Sci. and Eng., 56 (1982) 143-156